Proceeding of the IEEE
International Conference on Robotics and Biomimetics
Dali, China, December 2019

Design and Simulation of an Accelerometer Allocation Scheme for Six-dimensional Acceleration Sensor

Zhiwei Wu, Yongjun Sun*⁻, Fenglei Ni, Yiwei Liu, Hong Liu

State Key Laboratory of Robotics and System
Harbin Institute of Technology
Harbin, Heilongjiang Province, China

760101865@qq.com, sunyongjun@hit.edu.cn

Abstract -In this paper, a novel spatial geometry of six-dimensional acceleration sensor(SDAS) is designed. And the sensor equation is calculated. The reliability of SDAS is improved by adding redundant line accelerometer. The GDOP(Geometric Dilution of Precision) index used in satellite navigation is introduced into SDAS for configuration evaluation. Compared with the classic cube configuration, the three indexes have improved significantly. The relationship between the output error of the SDAS and the installation error of the linear accelerometer is analyzed theoretically. Compared with the proposed layout structure using 12 accelerometers, it has obvious advantages.

Index Terms - Six dimensional acceleration sensor; Sensor equation; GDOP; Error analysis.

I. INTRODUCTION

Acceleration sensors are increasingly used in automobile, medical, aerospace, robot control and other industries [1-4]. In reference [5], the acceleration sensor is used to perceive the vibration of the manipulator when it comes into contact with the target object, and the grasping action of the manipulator is remotely controlled to improve the success rate of the manipulator in grasping the target object.

In order to measure angular acceleration, six-dimensional acceleration sensors(SDAS) can be divided into two categories according to whether gyroscopes are used or not. The gyro free inertial measurement system has better performance, such as impact resistance, good thermal stability, high bandwidth and fast dynamic response, etc [6, 7]. Reference [8] believes that gyro-free SDAS will be the mainstream sensor in the future.

According to the measurement principle, SDAS without gyro can be divided into three types: one-piece structure, combined structure and parallel mechanism [9]. The basic principle of one-piece structure is spring-mass-damping structure [10]. The essence of the study of the combined structure is the geometric distribution or constraints of different linear accelerometers in space. The composite type does not require complex mechanical structure, high-precision sensitive elements, nor does it involve complex rigid body dynamics model. Combined sensor's advantage is to avoid the risk of differential operation with high frequency noise, using the mature uniaxial acceleration sensor technology, so you can according to different working conditions using different uniaxial acceleration sensor, but also has low cost, energy consumption province, long life, fast startup, angular velocity and angular acceleration measurement range, easy to maintain and repair, etc [11]. However, the combined accelerometer requires very high accuracy of the installation position and direction of each accelerometer, which is difficult to achieve in engineering. In addition, there are certain errors in the manufacturing process of each linear accelerometer, which are different from each other, making subsequent calibration more difficult. Therefore, it is particularly important to design a reasonable configuration. Even if there is installation position error and direction error, the measurement error of six-axis acceleration is still very small, and the error can be reduced through error compensation, so as to ensure the accuracy [12].

The combined structure of SDAS include cube configurations [13], 2-2-2 configurations, coplanar configuration [14], cylindrical configurations [15], etc. For the layout structure of 6 accelerometers, the minimum accelerometer is used to reduce the cost, but the integration calculation in the calculation process will bring cumulative errors, and there is no redundancy and poor reliability. Therefore, this paper proposes a new configuration based on the spherical layout structure of the twelve accelerometer, which increases the redundancy, and uses the redundant information to avoid integral calculation and effectively suppress the iteration error.

II. DESIGN OF SIX-DIMENSIONAL ACCELERATION SENSOR

A. Structural Design

In this paper, a spherical layout structure of twelve accelerometers is presented, as shown in Fig. 1. The structure in the figure is composed of 6 double-axis accelerometers, XYZ coordinate system represents the sensor coordinate system, and the solid line with black arrows represents the

sensitive axis direction of the linear accelerometer. In order to avoid loss of generality, the linear accelerometer with n sensitive axes is regarded as n linear accelerometers, and is represented by A1 to A12.

The linear accelerometer with spherical spatial arrangement is uniformly distributed and completely symmetrical. 6 double axis accelerometer distribution at the center of the cube's six faces, each line on the surface of the accelerometer's sensitive axis parallel to the surface, and the two directions by 90°. The origin of the coordinate system of the SDAS coincides with the center of the sphere, and the X, Y and Z axes are parallel to the cube edges. Let the sides of the cube be 2a.Then the direction and position of the sensitive axis of the linear accelerometer are shown in Table I.
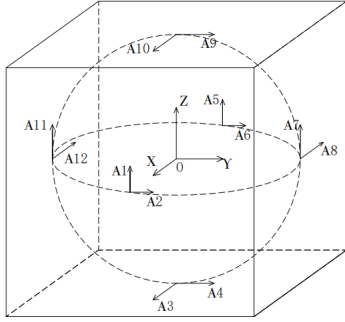

Fig. 1 Spatial geometry of 12 linear accelerometers

TABLE I
POSITION AND DIRECTION OF LINEAR ACCELEROMETER

Sensor number	The position vector	Sensitive axis direction
A1	$[a\ 0\ 0]^T$	$[0\ 0\ 1]^T$
A2	$[a\ 0\ 0]^T$	$[0\ 1\ 0]^T$
A3	$[0\ 0\ \text{-}a]^T$	$[1\ 0\ 0]^T$
A4	$[0\ 0\ \text{-}a]^T$	$[0\ 1\ 0]^T$
A5	$[\text{-}a\ 0\ 0]^T$	$[0\ 0\ 1]^T$
A6	$[\text{-}a\ 0\ 0]^T$	$[0\ 1\ 0]^T$
A7	$[0\ a\ 0]^T$	$[0\ 0\ 1]^T$
A8	$[0\ a\ 0]^T$	$[\text{-}1\ 0\ 0]^T$
A9	$[0\ 0\ a]^T$	$[0\ 1\ 0]^T$
A10	$[0\ 0\ a]^T$	$[1\ 0\ 0]^T$
A11	$[0\ \text{-}a\ 0]^T$	$[0\ 0\ 1]^T$
A12	$[0\ \text{-}a\ 0]^T$	$[\text{-}1\ 0\ 0]^T$

B. Calculation of Sensing Equation

The position vector of the 12 linear accelerometers in the sensor coordinate system is $r_i \in R_i^{3\times1}(i=1, 2\ldots12)$, then the position matrix of the linear accelerometer is (1):

$$r = \begin{bmatrix} a & a & 0 & 0 & -a & -a & 0 & 0 & 0 & 0 & 0 & 0 \\ 0 & 0 & 0 & 0 & 0 & 0 & a & a & 0 & 0 & -a & -a \\ 0 & 0 & -a & -a & 0 & 0 & 0 & 0 & a & a & 0 & 0 \end{bmatrix} \quad (1)$$

If the sensitive axis direction of the linear accelerometer in the sensor coordinate system is $u_i=[u_{ix}\ u_{iy}\ u_{iz}]^T \in R_i^{3\times1}(i=1, 2\ldots12)$, then the sensitive axis direction matrix is (2):

$$u = \begin{bmatrix} 0 & 0 & 1 & 0 & 0 & 0 & 0 & \text{-}1 & 0 & 1 & 0 & \text{-}1 \\ 0 & 1 & 0 & 1 & 0 & 1 & 0 & 0 & 1 & 0 & 0 & 0 \\ 1 & 0 & 0 & 0 & 1 & 0 & 1 & 0 & 0 & 0 & 1 & 0 \end{bmatrix} \quad (2)$$

The angular velocity coupling term is treated as an unknown variable. This method can effectively avoid the cumulative error caused by integration, and the algorithm is easier to implement, thus obtaining the output equation of the SDAS (3). A_i represents the output of the accelerometer.

$$\begin{bmatrix} A_1 \\ A_2 \\ \vdots \\ A_{12} \end{bmatrix} = \begin{bmatrix} J_{ACC1}^T & J_{ACC2}^T & J_{ACC3}^T \end{bmatrix} \begin{bmatrix} P_b'' + g \\ w_b' \\ vec(\Omega_b^2) \end{bmatrix} \quad (3)$$

$$J_{ACC1} = \begin{bmatrix} u_1 & u_2 & \cdots & u_{12} \end{bmatrix} \quad (4)$$

$$J_{ACC2} = \begin{bmatrix} -R_1^T u_1 & -R_2^T u_2 & \cdots & -R_{12}^T u_{12} \end{bmatrix} \quad (5)$$

$$J_{ACC3} = \begin{bmatrix} u_1 \otimes r_1 & u_2 \otimes r_2 & \cdots & u_{12} \otimes r_{12} \end{bmatrix} \quad (6)$$

Where $\otimes$ is the Kronecker multiplication [16], R_i is the antisymmetric matrix for r_i . Ω_b^2 is the antisymmetric matrix for w_b.

$$\Omega_b^2 = \begin{bmatrix} -(w_{by}^2 + w_{bz}^2) & w_{bx}w_{by} & w_{bx}w_{bz} \\ w_{bx}w_{by} & -(w_{bx}^2 + w_{bz}^2) & w_{by}w_{bz} \\ w_{bx}w_{by} & w_{bx}w_{bz} & -(w_{bx}^2 + w_{by}^2) \end{bmatrix} \quad (7)$$

$$J_{ACC} = \begin{bmatrix} J_{ACC1}^T & J_{ACC2}^T & J_{ACC3}^T \end{bmatrix} \quad (8)$$

After further mathematical calculation, the output equation (9) and configuration matrix (10) of the SDAS can be obtained as follows:

$$\begin{bmatrix} P_b'' + g \\ w_b' \\ w_{bx}w_{by} \\ w_{bx}w_{bz} \\ w_{by}w_{bz} \end{bmatrix} = (J_{ACC}^T J_{ACC})^{-1} J_{ACC}^T \begin{bmatrix} A_1 \\ A_2 \\ \cdots \\ A_{12} \end{bmatrix} \quad (9)$$

$(J_{ACC}^T J_{ACC})^{-1} J_{ACC}^T =$

$$\begin{bmatrix}
0 & 0 & \frac{1}{4} & 0 & 0 & 0 & 0 & -\frac{1}{4} & 0 & \frac{1}{4} & 0 & -\frac{1}{4} \\
0 & \frac{1}{4} & 0 & \frac{1}{4} & 0 & \frac{1}{4} & 0 & \frac{1}{4} & 0 & 0 & 0 \\
\frac{1}{4} & 0 & 0 & 0 & \frac{1}{4} & 0 & \frac{1}{4} & 0 & 0 & 0 & \frac{1}{4} & 0 \\
0 & 0 & 0 & \frac{1}{4a} & 0 & 0 & \frac{1}{4a} & 0 & -\frac{1}{4a} & 0 & -\frac{1}{4a} & 0 \\
-\frac{1}{4a} & 0 & -\frac{1}{4a} & 0 & 0 & 0 & 0 & 0 & 0 & \frac{1}{4a} & 0 & 0 \\
0 & \frac{1}{4a} & 0 & 0 & 0 & -\frac{1}{4a} & 0 & \frac{1}{4a} & 0 & 0 & 0 & -\frac{1}{4a} \\
0 & \frac{1}{4a} & 0 & 0 & 0 & -\frac{1}{4a} & 0 & -\frac{1}{4a} & 0 & 0 & 0 & \frac{1}{4a} \\
\frac{1}{4a} & 0 & -\frac{1}{4a} & 0 & -\frac{1}{4a} & 0 & 0 & 0 & 0 & \frac{1}{4a} & 0 & 0 \\
0 & 0 & 0 & -\frac{1}{4a} & 0 & 0 & \frac{1}{4a} & 0 & \frac{1}{4a} & 0 & -\frac{1}{4a} & 0
\end{bmatrix} \quad (10)$$

It can be seen from the output equation that the number of unknown variables is 9, while the number of the line accelerometer is 12, so the equation has solutions. The above method is to use the inverse theory of generalized inverse matrix and observe the generalized inverse matrix (10). It can be seen that the decoupling of angular acceleration is related

to the value of spatial geometric configuration size a. In fact, the decoupling of 3d linear accelerometer is to calculate the average value of the output of the corresponding linear accelerometer.

C. Configuration Evaluation

The GDOP index is used to reflect the influence of system configuration design on the solution accuracy [17, 18]. The smaller the GDOP index is, the higher the positioning accuracy is. Ignoring the influence of random noise of linear accelerometer, let the measurement error of N accelerometers be (11) and the error vector of solution be(12), where J^{-1}_{ACC} is the generalized inverse obtained by (10) .

$$\Delta f = \left[\Delta f_1 \cdots \Delta f_N\right]^T \tag{11}$$

$$\Delta y = \left[\left(\Delta p_b''\right)^T \quad \left(\Delta w_b'\right)^T\right]^T = J^{-1}_{ACC}\Delta f \tag{12}$$

$$J^{-1}_{ACC} = \left(J^T_{ACC}J_{ACC}\right)^{-1}J^T_{ACC} \tag{13}$$

GDOP is the amplification factor of the measurement error of the accelerometer to the error of the solution of angular velocity and linear acceleration, and (14) can be obtained according to its definition.

$$GDOP = \frac{\sigma_{\Delta y}}{\sigma_{\Delta f}} = \sqrt{trace\left(J^T_{ACC} \cdot J_{ACC}\right)^{-1}} \tag{14}$$

$$J_{ACC} = \left[J^T_{ACC1} J^T_{ACC2}\right] \tag{15}$$

Therefore, the diffusion factors of angular acceleration and linear acceleration are introduced, as shown in (16) and (17) :

$$p''GDOP = \sqrt{trace(J^T_{ACC1}J_{ACC1})^{-1}} \tag{16}$$

$$w'GDOP = \sqrt{trace(J^T_{ACC2}J_{ACC2})^{-1}} \tag{17}$$
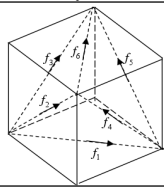
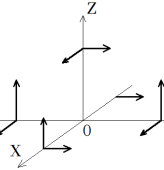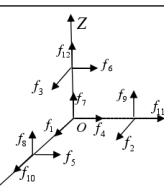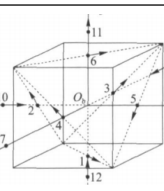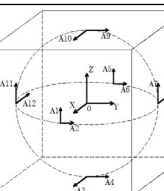$$J_{ACC2} = \frac{J_{ACC2}}{a} \tag{18}$$

In order to exclude the influence of size parameters, dimensions of each submatrix must be unified in the matrix $J_{ACC}=[J^T_{ACC1} \ J^T_{ACC2}]$, and dimensionless transformation of J_{ACC2} is required, as shown in (18). Matlab is used to calculate the spherical accelerometer layout structure proposed in this paper, and three GDOP indexes are solved. The calculation results and several acceleration configurations are shown in Table II.

It can be seen from table II that p"GDOP index is related to the number of linear accelerometers, the more the number, the smaller the p"GDOP value, and the more accurate the measurement. The w"GDOP index is related to the linear accelerometer layout, and all indexes of the spherical layout of the 12 accelerometers proposed in this paper are obviously better than those of the cube layout. Compared with the layout of the same number of linear accelerometers, the w"GDOP value and the GDOP value are both smaller and the layout is more reasonable.

From the perspective of geometric space, the spherical structure proposed in this paper belongs to a completely

symmetrical configuration, and the linear accelerometer is evenly distributed. This configuration is suitable for mounting on the surface of a spherical structure or at the center of a surface of a cube structure.

TABLE II
GDOP INDEXES OF DIFFERENT ACCELEROMETER CONFIGURATIONS

Configuration	Linear accelerometer layout	p"GDOP	w"GDOP	GDOP
Six accelerometer cube layout[13]		1.2247	1.2247	1.7321
Nine accelerometer space arrangement[15]		1.0000	1.0408	1.6073
Twelve accelerometer space arrangement[19]		0.8660	1.2247	1.7748
Another twelve accelerometer layout structure[20]		0.8860	1.2247	1.5
Twelve accelerometer spherical arrangement		0.8660	0.8660	1.2247

D. Redundancy Analysis

According to (9), there are 9 unknown variables in the sensor decoupling system, so at least 9 linear accelerometers are needed to solve this equation. In order to improve the sensor stability and anti-interference ability, a redundant line accelerometer is added in each direction. In order to explore the influencing factors of the output of accelerometers on each line, equation (19) can be obtained from equation (3). According to the sensitive axis direction of the line accelerometer, the 12 line acceleration plans can be divided into three groups of X, Y and Z axis directions, as shown in Table III. There are 3 unknown variables and 4 linear accelerometers in each group, so there is 1 redundant linear accelerometer in each group. According to the principle of permutation and combination, the combination of solutions of unknown variables in each group is 4, and the number of combinations of equations for the final solution is 64. Therefore, the redundancy of spherical space geometry

proposed in this paper improves the reliability of the system and provides a possibility for fault detection and isolation.

$$
\begin{cases}
A_1 = p''_{bz} - aw'_{by} + aw_{bx}w_{bz} \\
A_2 = p''_{by} + aw'_{bz} + aw_{bx}w_{by} \\
A_3 = p''_{bx} - aw'_{by} - aw_{bx}w_{bz} \\
A_4 = p''_{by} + aw'_{bx} - aw_{by}w_{bz} \\
A_5 = p''_{bz} + aw'_{by} - aw_{bx}w_{bz} \\
A_6 = p''_{by} - aw'_{bz} - aw_{bx}w_{by} \\
A_7 = p''_{bz} + aw'_{bx} + aw_{by}w_{bz} \\
A_8 = -p''_{bx} + aw'_{bz} - aw_{bx}w_{by} \\
A_9 = p''_{by} - aw'_{bx} + aw_{by}w_{bz} \\
A_{10} = p''_{bx} + aw'_{by} + aw_{bx}w_{bz} \\
A_{11} = p''_{bz} - aw'_{bx} - aw_{by}w_{bz} \\
A_{12} = -p''_{bx} - aw'_{bz} + aw_{bx}w_{by}
\end{cases} \tag{19}
$$

TABLE III
REDUNDANCY ANALYSIS OF SIX-DIMENSIONAL ACCELERATION SENSOR

Direction	Linear accelerometer	The unknown variables	Redundancy
X	A3 A8 A10 A12	p''_{bx}	4
		$w'_{by} + w_{bx}w_{bz}$	
		$w'_{bz} - w_{bx}w_{by}$	
Y	A2 A4 A6 A9	p''_{by}	4
		$w'_{bz} + w_{bx}w_{bz}$	
		$w'_{bx} + w_{by}w_{bz}$	
Z	A1 A5 A7 A11	p''_{bz}	4
		$w'_{by} - w_{bx}w_{bz}$	
		$w'_{bx} + w_{by}w_{bz}$	

III. ERROR ANALYSIS

A. Analysis of Installation Error

The installation error of the linear accelerometer not only affects the output of the linear accelerometer, but also affects the configuration matrix of the SDAS. Ideally, r_i is installed vector, u_i is the sensitive axis vector, assuming that $\Delta r_i = [\Delta r_{ix} \ \Delta r_{iy} \ \Delta r_{iz}]^T$ is the actual sensor installation error vector, $\Delta u_i = [\Delta \alpha_i \Delta \beta_i]^T$ is the sensitive axis error. $\Delta \alpha_i$ is the error in the plane of the sensitive axis, $\Delta \beta_i$ is the error outside the plane of the sensitive axis, so we can get (20), a_{ri} is the line of the actual output of the accelerometer, a_i is the ideal linear accelerometer output, ΔR_i is the antisymmetric matrix of Δr_i.

$$
a_{ri} = J_r \begin{bmatrix} p''_b + g \\ w'_b \end{bmatrix} + (c_i + \Delta c_i)vec(\Omega_b^2) \tag{20}
$$

$$
J_r = \begin{bmatrix} u_i^T + \Delta u_i^T & -(u_i^T R_i + u_i^T \Delta R_i + \Delta u_i^T R_i + \Delta u_i^T \Delta R_i) \end{bmatrix} \tag{21}
$$

$$
c_i + \Delta c_i = \left[vec(u_i r_i^T) \right]^T + \left[vec(\Delta u_i r_i^T) \right]^T \\
+ \left[vec(u_i \Delta r_i^T) \right]^T + \left[vec(\Delta u_i \Delta r_i^T) \right]^T \tag{22}
$$

$$
a_i = \begin{bmatrix} u_i^T & -u_i^T R_i \end{bmatrix} \begin{bmatrix} p''_b + g \\ w'_b \end{bmatrix} + u_i^T \Omega_b^2 r_i \tag{23}
$$

Ignore the higher order terms and its acceleration coupling term. The output error a_{ei} of the line accelerometer is shown in (24).

$$
a_{ei} = a_{ri} - a_i \approx \begin{bmatrix} \Delta u_i^T & -\Delta u_i^T R_i - u_i^T \Delta R_i \end{bmatrix} \begin{bmatrix} p''_b + g \\ w_b \end{bmatrix} \tag{24}
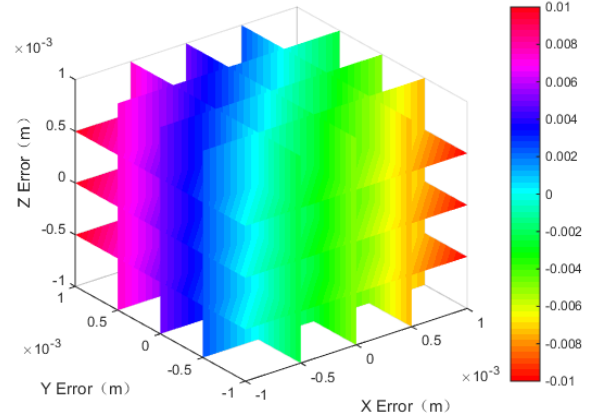$$

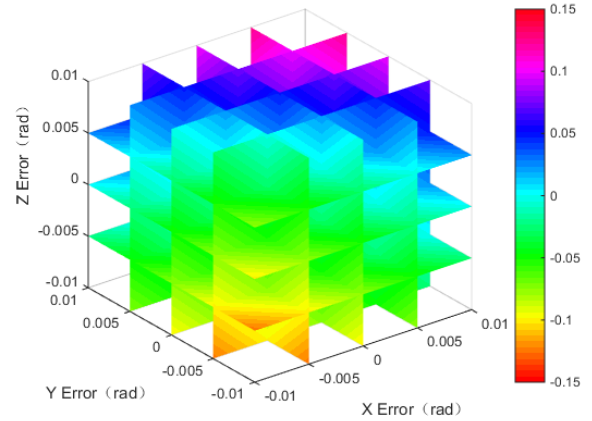Fig. 2 Relation between position error and output error

Fig. 3 Relation between direction error of sensitive axis and output error

Taking linear acceleration A1 as example. Take the variation range of dimension parameter a as 35±1mm. When the linear acceleration and angular acceleration are the constant inputs of 5m/s² and 5rad/s², respectively, draw the four-dimensional slice graph of the output error of the linear accelerometer that only considers the installation error of position and that only considers the installation error of sensitive axis. As shown in Fig. 2, the three axes in the figure respectively represent the variation of three position errors, with a range of ±1mm. In order to intuitively express the relationship between the output error and the direction error of the sensitive axis, the direction cosine is used to express the direction of the sensitive axis of the linear accelerometer in the sensor coordinate system. As shown in Fig. 3, the three axes in the figure respectively represent the variation of the directional errors of the three sensitive axes. The variation range is ±0.01rad. The color indicates that the output error unit of the line accelerometer is m/s². By comparing Fig. 2 with Fig. 3, it can be seen that the direction error of the sensitive

axis has a great influence on the output error of linear acceleration.

In Simulink, we use 1Hz sinusoidal excitation as input to analyze the influence of installation error of linear accelerometer on output of linear accelerometer, and the installation error and sensitive axis direction error of outgoing linear accelerometer were randomly given. The amplitude of linear acceleration in the direction of XYZ is 0.1m/s², 0.5m/s² and 0.2m/s² respectively. The amplitude of angular acceleration in the direction of XYZ is 10rad/s², 5rad/s² and 5rad/s² respectively. Take accelerometers from line A1 to A4 for example, their output errors are shown in Fig. 4.

a) Relationship between installation error and output error

b) Relationship between position error and output error

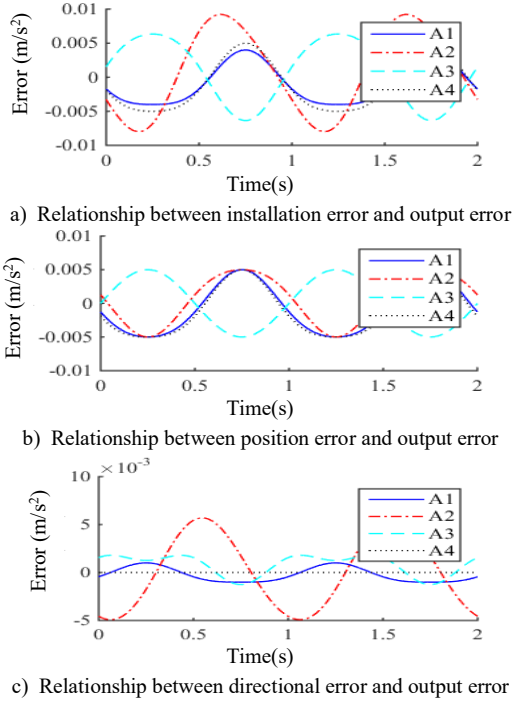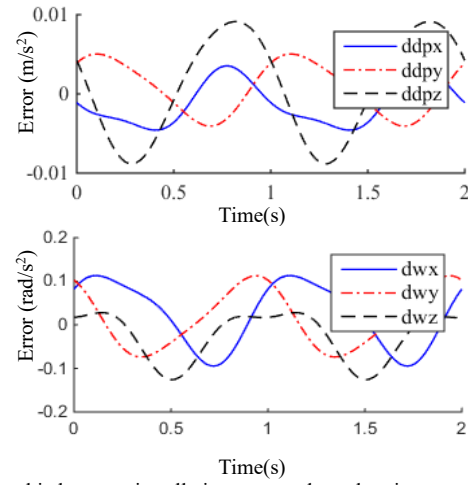c) Relationship between directional error and output error

Fig. 4 Relationship between installation error and output error of linear accelerometer

B. Analysis of Measurement Error

The measurement error formula of the SDAS is shown in (25).

$$\begin{bmatrix} \Delta p_b'' \\ \Delta w_b' \end{bmatrix} = J^{-1} \begin{bmatrix} a_{r1} \\ a_{r2} \\ \vdots \\ a_{r12} \end{bmatrix} - J^{-1} \begin{bmatrix} a_1 \\ a_2 \\ \vdots \\ a_{12} \end{bmatrix} = J^{-1} \begin{bmatrix} a_{e1} \\ a_{e2} \\ \vdots \\ a_{e12} \end{bmatrix} \quad (25)$$

In order to simulate the influence of installation error on six-axis acceleration measurement error, we adopted 1Hz sinusoidal excitation as input, and the specific parameters are the same as in the previous section. The simulation results are shown in Fig. 5.

a) Relationship between installation error and acceleration measurement error
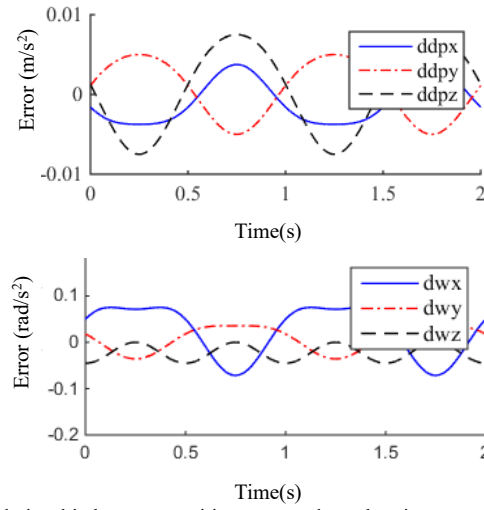
b) Relationship between position error and acceleration measurement error
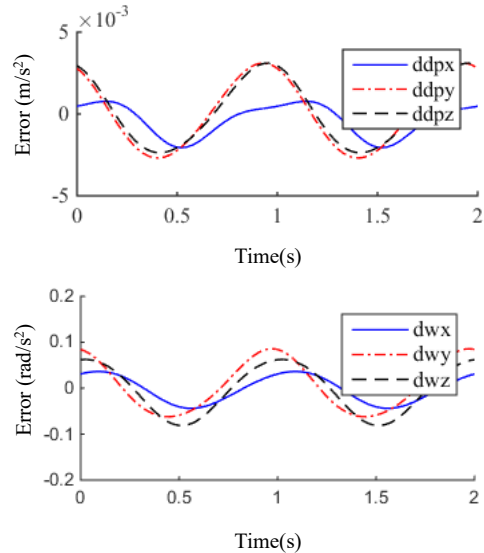
c) Relationship between directional error and acceleration measurement error

Fig. 5 Relationship between installation error and measurement error

It can be seen from Fig. 5 that the influence of installation error on diagonal acceleration measurement error is greater than that on linear acceleration measurement error. The

influence of position error is greater than that of sensitive axis direction error. Among them, the influence of the direction error of the sensitive axis on the linear acceleration measurement error is especially small.
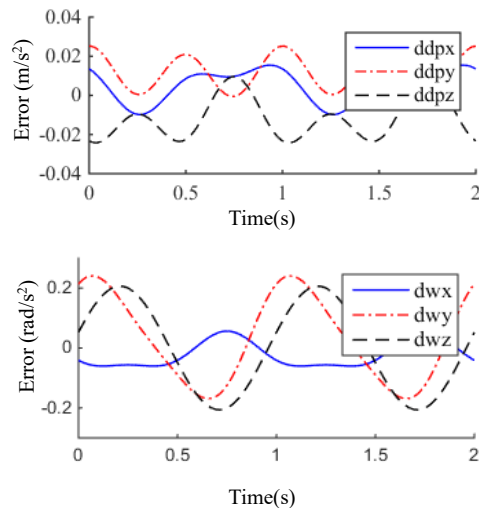

Fig. 6 Analysis of the layout structure of another twelve accelerometer

The same methods and parameters are used to analyze the installation error of another 12 accelerometer layout structure proposed by Wang Xiaona [20], and the results are shown in Fig. 6. Compared with Fig. 5 a), the installation error of the configuration proposed in this paper has less influence on the acceleration measurement.

IV. CONCLUSION

This paper presents a layout structure using 12 linear acceleration sensors. Compared with other 12 accelerometer layout structures, it has a smaller GDOP value, so the measurement accuracy is higher. In the XYZ axis, the redundancy of the sensor is reasonably distributed and the waste is reduced. The results of error analysis show that the installation error of the linear accelerometer in this configuration has little influence on the measurement of linear acceleration and angular acceleration. It can be applied to robotic arms for direct acceleration control, vibration suppression, parameter identification, sensor calibration, sensor information fusion, delay compensation, and tactile recurrence. However, for the production of sensor prototype, calibration experiment research and error compensation research need to be completed in the future.

REFERENCES

[1] Cucci D A, Crespillo O G, Khaghani M. An analysis of a gyro-free inertial system for INS/GNSS navigation[C]// European Navigation Conference. 2016.
[2] Li Chenggang, Chen Jing, You Jingjing, et al. Fault Diagnosis and Restoration for Parallel Type Six-axis Accelerators[J]. Journal of Vibration and Shock, 2017, 36(15):222-229.
[3] Satoshi Tsuji, Teruhiko Kohama. Using a convolutional neural network to construct a pen-type tactile sensor system for roughness recognition[J]. Sensors and Actuators A, 2019, 291:7-12.
[4] Ali A A, Mahmood W S. Active Vibration Suppression of Aerobatic Aircraft Wing by Acceleration Feedback Controller[J]. International Journal of Computer Appli cations, 2017, 157(10).

[5] Khurshid R, Fitter N, Fedalei E, et al. Effects of Grip-Force, Contact, and Acceleration Feedback on a Teleoperated Pick-and-Place Task[J]. IEEE Transactions on Haptics, 2016, 10(1):40-53.
[6] Edwan E, Knedlik S, Loffeld O. Constrained Angular Motion Estimation in a Gyro-Free IMU[J]. IEEE Transactions on Aerospace & Electronic Systems, 2011, 47(1):596-610.
[7] Ph. Zhuravlev1, S. Perelyaev, et al. Strapdown Inertial Navigation System of Minimum Dimension[C]// 2018 DGON Inertial Sensors and Systems, 2018.
[8] Naseri H, Homaeinezhad M R. Improving measurement quality of a MEMS-based gyro-free inertial navigation system[J]. Sensors & Actuators A Physical, 2014, 207(3):10-19.
[9] You Jing-jing, Li Cheng-gang, Zuo Fei-yao, et. al. Current studying status and developing trend of six-axis accelerometers[J]. Journal of Vibration and Shock, 2015(11):150-159.
[10] Zhibo S, Jinhao L, Chunzhan Y, et al. A Small Range Six-Axis Accelerometer Designed with High Sensitivity DCB Elastic Element[J]. Sensors, 2016, 16(9):1552-.
[11] Liu Zhiping, Hao Yanling, et al. Research on Several Key Technologies of GFSINS[D]. Harbin Engineering University, 2010.
[12] Yang, Ming, Liu, Ming, et al. Research on the GFSINS/GPS/CNS integrated navigation technology for hypersonic vehicle[C]// 21st AIAA International Space Planes and Hypersonics Technologies Conference, Hypersonics 2017.
[13] Chen J H, Lee S C, Debra D B. Gyroscope free strapdown inertial measurement unit by six linear accelerometers[J]. Journal of Guidance, Control, and Dynamics, 1994, 17(2):286-290.
[14] Yuan Gang, Wang Daihua. Principle, System, and Characteristics of a Six Degree-of-Freedom Accelerometer[D]. Chongqing University, 2010.
[15] Zou T, Ni F, Guo C, et al. Design of 6-DOF accelerometer and application in impedance control of manipulators with flexible joints[C]// IEEE International Conference on Robotics & Biomimetics. IEEE, 2017.
[16] Harville D A. Matrix algebra from a statistician's perpsetive[M]. New York:Spring, 1997: 333−343.
[17] Aggarwal P, Syed Z, Niu X, et al. A standard testing and calibration procedure for low cost MEMS inertial sensors and units[J]. Journal of navigation, 2008, 61(02): 323−336.
[18] Parente C, Meneghini C. Advantages of Multi GNSS Constellation: GDOP Anal ysis for GPS, GLONASS and Galileo Combinations[J]. International Journal of Engineering and Technology Innovation, 2016, 7(1): 1−10.
[19] Schopp P, Klingbeil L, Peters C, et al. Sensor fusion algorithm and calibration for a gyroscope-free IMU[J]. Procedia Chemistry, 2009, 1(1): 1323−1326.
[20] Wang Xiaona, Wang Shuzong, Zhu Huabing, et al. Study on Models of Gyroscope-free Strap-down Inertial Navigation System[J]. Acta Armamentarii, 2006, 27(2).